

# Analysis of the $\alpha$ to $\beta$ phase transformation in Y–Si–Al–O–N ceramics

P. A. WALLS, M. UEKI

*Advanced Materials and Technology Research Laboratories, Nippon Steel Corporation, 1618 Ida, Nakahara-ku, Kawasaki 211, Japan*

The  $\alpha$  silicon nitride– $\beta$  sialon phase transformation in the Y–Si–Al–O–N system was investigated by transmission and scanning electron microscopy and X-ray diffractometry using samples which contained up to 40% liquid-forming components at temperatures between 1500 and 1600 °C. Completely dense samples suitable for TEM analysis, in which the  $\alpha$  to  $\beta$  transformation could be examined, were prepared using hold times as short as 5 min under a nominal uniaxial pressure followed by rapid cooling. Spheroidal, partially dissolved,  $\alpha$  silicon nitride grains, together with acicular grains of  $\beta$  sialon, were observed in a glass phase containing a very low nitrogen content (undetectable by electron microprobe analysis). This absence of nitrogen build-up in the liquid phase between the dissolution and precipitation sites during the  $\alpha$  to  $\beta$  transformation indicates that the diffusion of nitrogen through the liquid phase is extremely rapid. Nucleation of the  $\beta$  sialon was almost entirely homogeneous and the unconstrained nature of the liquid environment resulted in growth of defect-free  $\beta$  sialon grains with curved growth fronts perpendicular to the  $c$ -axis. The technique described allows direct observation of the effect of various additives on the  $\alpha$  to  $\beta$  phase transformation.

## 1. Introduction

There are basically three stages to the densification process which occurs during the liquid-phase sintering of ceramic materials [1]. These are initial particle rearrangement, a second stage in which material is transported either by diffusion at the contact point of neighbouring grains or by a dissolution–reprecipitation process in the liquid phase and finally by elimination of closed porosity. In the second stage, the growth of material is controlled either by the rate at which atoms leave or enter the solid/liquid interface, or by the rate at which the dissolved atoms diffuse through the liquid. The kinetics of the dissolution–reprecipitation process are determined by such factors as the composition and amount of liquid phase present at the sintering temperature and the heating pattern used. This, in turn, influences the microstructure and hence mechanical properties of silicon nitride-based ceramics.

Most commercially produced silicon nitride ceramics contain less than 15 vol% grain-boundary glassy phase and hence low volume fractions of liquid phase during sintering. When the volume fraction of liquid is low, the theoretical analysis proposed by Wagner [2] for grain growth by dissolution–reprecipitation processes must be amended. Ardell [3] showed that by using an adjusted rate constant which takes into account the volume fraction of liquid present, when the proportion of liquid is small, the two growth processes yield very similar particle-size distributions. This assumes non-touching conditions and

also that the precipitated material is spherical in nature.

In real materials, e.g. low-oxide additive content  $\beta$  sialon ceramics where the liquid phase is minimal, frequent grain contact must be assumed and there is the additional complicating factor of a preferential growth direction parallel to the  $c$ -axis of the  $\beta$  unit cell. This makes theoretical modelling extremely difficult and indicates the need for some basic data on the kinetics and form of the  $\alpha$  to  $\beta$  transformation. Although a significant volume of research has been conducted into the densification and transformation mechanisms which occur during sintering in such ceramics [4–10], the  $\alpha$  to  $\beta$  transformation has never been directly imaged using high-magnification transmission electron microscopy. Investigation of the dissolution–reprecipitation process at relatively low temperatures (1500–1600 °C) with short hold times (5–30 min) at temperature by TEM is extremely difficult for low glass content silicon nitride ceramics, due to formation of highly porous and hence low-strength sintered material from which preparation of good TEM samples is virtually impossible. Sufficiently dense samples for TEM can be obtained by sintering at temperatures as low as 1500 °C with just a 5 min hold at temperature if approximately 40% liquid-forming components are incorporated into the material. This high liquid and hence glass content also separates the reactant  $\alpha$  silicon nitride from the precipitating  $\beta$  sialon which makes analysis of precipitation sites and rate of dissolution and pre-

precipitation easier. Samples with a composition situated between the  $\beta$  sialon and glass-forming phase regions of the Y-Si-Al-O-N system were prepared and analysed.

## 2. Experimental procedure

Three compositions (A, B and C) consisting of high glass content  $\beta$  sialon materials were prepared by mixing  $\alpha$  silicon nitride (Ube SN E-10), alumina (Sumitomo chemicals, AKP-50), yttria (Nippon yttrium Co.) and silica (Nipsil) powders in a ratio which, under high-temperature equilibrium conditions, i.e. 1750 °C for 1 h, would yield 50:50, 60:40 and 80:20 mixtures of  $\beta$  sialon and Y-sialon glass, respectively. The compositions investigated are shown in Table I. Fig. 1 shows the quaternary behaviour diagram of the Y-Si-Al-O-N system at 1750 °C, with the positions of sample B shown, together with the relative positions of the  $\beta$  sialon and glass-forming regions.

The reagents were mixed in a silicon nitride ball mill using media of the same material and acetone as the

mixing medium. After drying the powder, 3 g, 18 mm diameter disc compacts were prepared by uniaxial pressing. These were inserted into a small hot-pressing graphite die with an outer diameter of 40 mm and inner bore of 20 mm. The compact was surrounded by BN powder to prevent reaction with the die. This assembly was then placed into a tungsten mesh element furnace and a pressure of 1 MPa was applied by a feedback-controlled hydraulic loading apparatus. Rapid heating and cooling rates of 100 °C min<sup>-1</sup> to and from heat-treatment temperatures between 1500 and 1600 °C with hold times between 5 and 80 min were used so that the  $\alpha$  to  $\beta$  transformation could be observed at various stages during the sintering process. Phase analysis was performed by CuK $\alpha$  X-ray diffractometry, referring to all 2 $\theta$  reflections between 10° and 80°, although in Fig. 6 (see later) only the section of the XRD traces between 30° and 40° are shown for simplification. Samples were thinned using an argon ion-beam miller for TEM observation and polished and plasma etched for SEM studies. Compositional analysis was performed using energy dispersive X-ray analysis (EDAX) in STEM mode with a windowless detector so that oxygen and nitrogen analysis could be performed.

TABLE I Composition of  $\beta$  sialon: glass composites investigated

Sample	Composition (wt %)				$\beta$ : glass ratio
	Si <sub>3</sub> N <sub>4</sub>	Y <sub>2</sub> O <sub>3</sub>	Al <sub>2</sub> O <sub>3</sub>	SiO <sub>2</sub>	
A	63.3	20.7	14.6	1.4	80:20
B	44.6	35.9	12.0	7.5	60:40
C	37.1	42.0	10.9	10.0	50:50

## 3. Results and discussion

### 3.1. Samples with different $\beta$ : glass ratios

Fig. 2 shows a scanning electron micrograph of a plasma-etched, low glass content  $\beta$  sialon material. The  $\beta$  grains are situated in a continuous Y-Si-Al-O-N glass phase of bright contrast. The

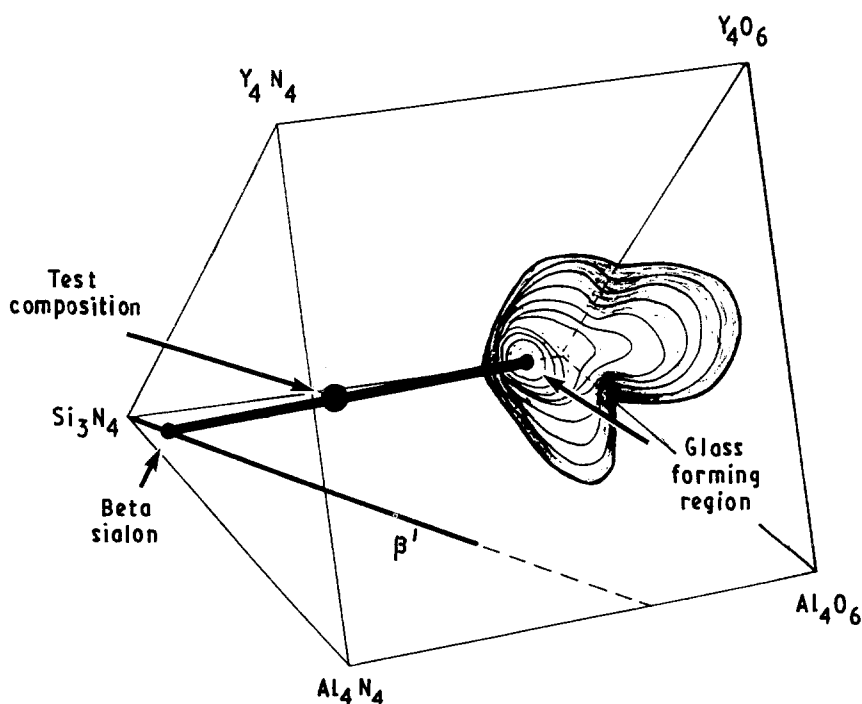


Figure 1 Relationships in the Y-Si-Al-O-N system.

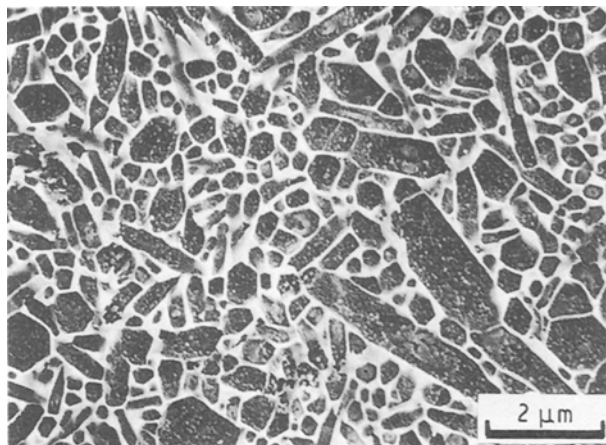


Figure 2 Scanning electron micrograph of a plasma-etched low glass content  $\beta$  sialon ceramic.

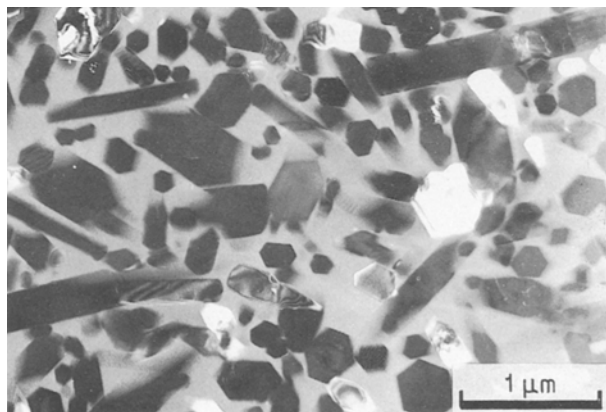


Figure 3 TEM dark-field image of Sample A hot pressed at 1600 °C for 1 h.

microstructure is typified by a bimodal grain size distribution with imperfect hexagonal grains formed by impingement of neighbouring grains during the growth stage of the sintering process. Even in higher glass content composites, for example Sample A, the 75:25  $\beta$  sialon: glass material shown in Fig. 3, where the “entrapped” grain phenomenon described by Hwang and Tien [7] is not prevalent, the microstructure is confused, making analysis difficult. Samples B and C, containing 50% and 40% glass-forming components, respectively, contain sufficient matrix phase to separate the reactants and products of the  $\alpha$  to  $\beta$  transformation to allow unimpeded analysis to be performed.

During heat treatment, the applied pressure was maintained at a low value (1 MPa) so that material was not extruded from the graphite jig, but was sufficient to obtain dense samples by preventing decomposition due to evolution of SiO and N<sub>2</sub> gases. Attempts to pressureless sinter such high liquid-forming compositions resulted in extremely bloated

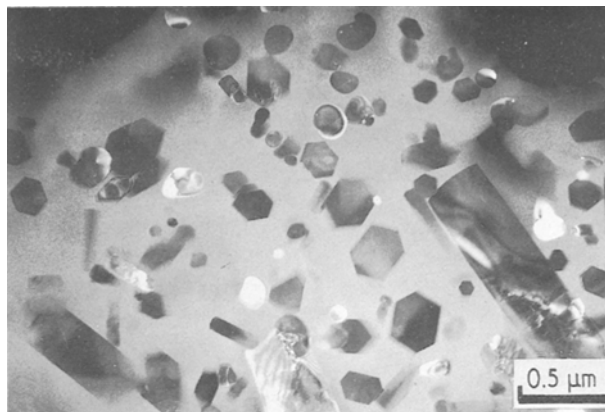
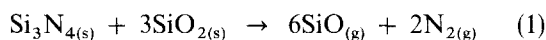


Figure 4 TEM dark-field image of Sample B hot pressed at 1600 °C for 10 min.

material which could not be analysed by TEM. The bloating, which has also been noted by Loehman [11] during preparation of high nitrogen content glasses, was a result of decomposition based on the reaction



Application of a uniaxial pressure to the sample during heat treatment can reduce the evolution of SiO and N<sub>2</sub> and so allow dense samples to be prepared.

Fig. 4 shows a dark-field TEM image (illuminated using the amorphous halo in the electron diffraction pattern) of Sample B, the 50:50,  $\beta$ :glass-forming composite. This sample was hot pressed at 1600 °C for 10 min and contains three distinct phases. The light-grey matrix is a Y-Si-Al-O-N glass, the (apparently) rectangular and hexagonal grains are sections through the acicular  $\beta$  sialon parallel and perpendicular to the *c*-axis and the rounded particles are  $\alpha$  silicon nitride. The specifications of the  $\alpha$  silicon nitride powder indicate that the maximum particle size is 3  $\mu\text{m}$  with a mean of 0.5  $\mu\text{m}$ . The particles shown in the micrograph and observed elsewhere in the sample were all under 0.5  $\mu\text{m}$ , indicating that a significant amount of dissolution had occurred. A higher magnification TEM image and corresponding X-ray spectra of the same sample are shown in Fig. 5. The rounded nature of the  $\alpha$  silicon nitride particles, which is due to the dissolution of silicon and nitrogen from the surface, indicates that there are no preferential dissolution sites, although the mottled contrast of the grain in the centre of the TEM image in Fig. 5a, may indicate some preferential dissolution on the atomic scale.

The EDAX spectrum shown in Fig. 5c indicates that the diffusion of nitrogen species through the liquid phase must be extremely rapid because the spectrum taken during point analysis of the glassy phase (analysis point marked by an asterisk) indicates an almost zero nitrogen content (N.B. the carbon peak results from the coating the sample was given to prevent charging during STEM analysis).

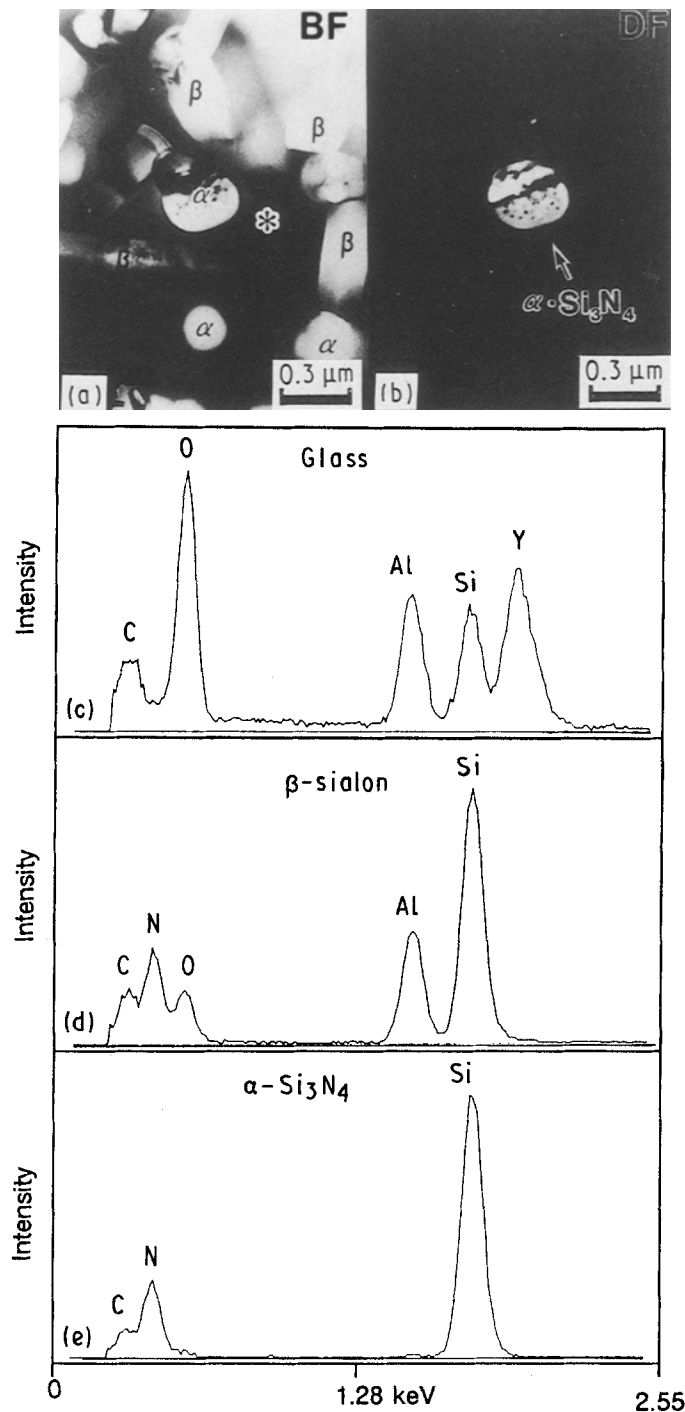


Figure 5 Sample C hot pressed at 1600 °C for 10 min. (a) Bright-field TEM image, (b) dark-field TEM image, (c) EDAX spectrum for the region marked with an asterisk, (d) EDAX spectrum for a  $\beta$  sialon grain, (e) EDAX spectrum for the rounded particle in (a) and (b).

### 3.2. Effect of heating time and temperature

Two hot-pressing temperatures, 1500 and 1600 °C, were selected, because they bound the temperature range in which  $\beta$  sialon is known to nucleate and grow [12]. The lowest temperature at which dense samples suitable for TEM analysis can be prepared is limited only by the eutectic temperature of the system in question. In this case, the eutectic temperature in the  $Y_2O_3$ - $Al_2O_3$ - $SiO_2$  system lies at approximately 1350 °C [13]. Once these three oxide components react, rapid liquid-phase densification can occur

by viscous flow leading to production of low-porosity samples containing non-equilibrium unreacted material.

The X-ray diffraction results for Sample B hot pressed at 1500 and 1600 °C with hold times between 5 and 80 min at temperature, are shown in Fig. 6. At 1500 °C, traces of  $\beta$  sialon were observed after only a 5 min hold. The majority of the  $\alpha$  silicon nitride had not dissolved in the liquid and densification had been achieved by viscous flow of the liquid phase formed by reaction of the oxide components. The  $\alpha/\beta$  ratio

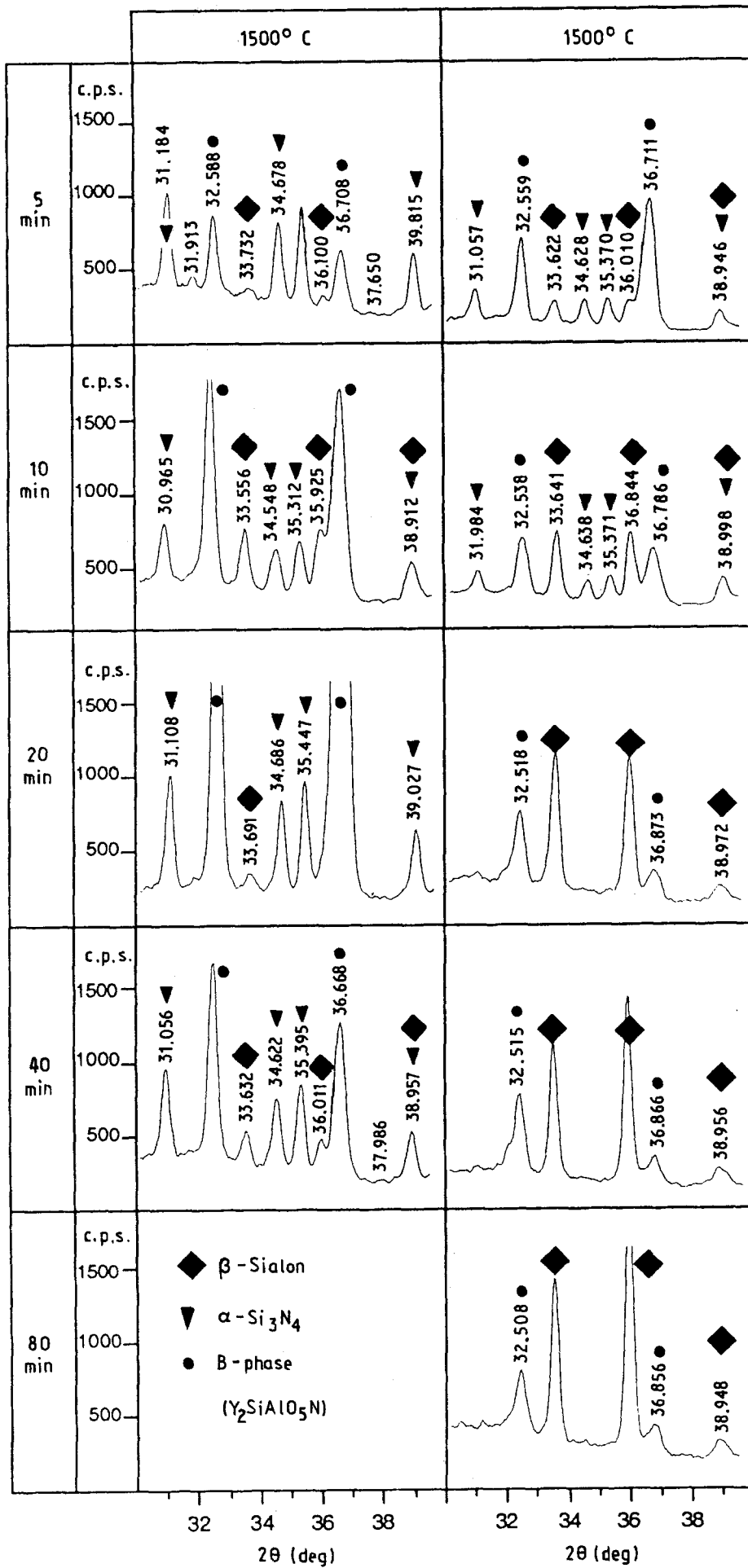


Figure 6 XRD traces of Sample C hot pressed at 1500 and 1600°C with hold times from 5–80 min.

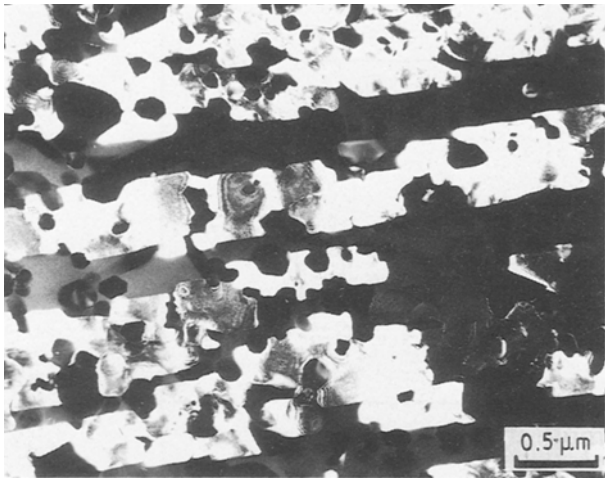


Figure 7 Dark-field transmission electron micrograph of B-phase crystallites in Sample C.

gradually decreased with time and after 40 min the proportion of  $\beta$  phase was greater than that of the  $\alpha$  silicon nitride reactant. The large peaks observed at  $32.5^\circ$  and  $36.7^\circ$   $2\theta$  are the (102) and (004) reflections corresponding to an aluminium-containing  $\alpha$ -wollastonite phase known as B-phase [14] which has a composition in the range  $Y_2SiAlO_5N$  to  $YSi_{0.3}Al_{0.7}O_{2.7}N_{0.3}$ . It has a hexagonal crystal nature and is situated in the glass-forming region of the Y-Si-Al-O-N system, hence its formation by devitrification can easily occur with very little atomic rearrangement. The high intensity of the (004) reflection indicates a high degree of preferential growth parallel to the  $c$ -axis of the B-phase crystallites. Boskovic and Kostic [15] noted that crystallization of the B-phase (termed by him as N-phase) occurred during slow cooling in the temperature range  $1100$ – $900^\circ\text{C}$ . A region containing partially devitrified B-phase is shown in Fig. 7, where a magnified region of the crystallite swarms, which measured up to  $100\ \mu\text{m}$  long, can be seen. The B-phase appears to have grown around both the dissolving  $\alpha$  silicon nitride and growing  $\beta$  sialon grains. The presence of  $\beta$  grains inside or partially penetrating the B-phase suggests that devitrification occurred during cooling even though the observed cooling rate was rapid ( $100^\circ\text{C}\ \text{min}^{-1}$ ) which suggests that the B-phase formation does not impede the  $\alpha$  to  $\beta$  transformation at the hold temperature.

At  $1600^\circ\text{C}$ , even with the shortest hold time at temperature (5 min), considerable  $\alpha$  silicon nitride had dissolved into the liquid phase and  $\beta$  sialon precipitated. With a 20 min hold at  $1600^\circ\text{C}$ , the  $\alpha$  silicon nitride had completely dissolved and the proportion of  $\beta$  sialon had greatly increased. These results agreed with the findings by one of the present authors [12], of the  $\beta$  sialon formation temperature between  $1500$  and

$1600^\circ\text{C}$ . The ratio of the intensities of the two strongest  $\beta$  sialon reflections at  $33.6^\circ$  and  $36.0^\circ$ , the (101) and (210) peaks, respectively,  $I_{101}:I_{210}$ , decreases as the hold time at temperature increases. This indicates an anisotropic nature of the growth of the  $\beta$  sialon grains, i.e. initially equiaxed, with an increase in the  $c/a$  aspect ratio after longer reaction times. B-phase is also present in these samples; however, the relative proportion is much less than in the samples heat treated at  $1500^\circ\text{C}$ . This is most probably related to the difference in liquid composition at the two temperatures, i.e. a reduced aluminium content at  $1600^\circ\text{C}$ .

Nucleation and growth of the  $\beta$  sialon and dissolution of the  $\alpha$  silicon nitride are shown in the TEM images in Fig. 8 for Sample C hot-pressed at  $1600^\circ\text{C}$ . These TEM data correlate well with the XRD results concerning the change in the  $c/a$  ratio of the  $\beta$  sialon with time. Nucleation of the  $\beta$  phase appears to have been completely homogeneous in the liquid phase formed by the reaction between the yttria, alumina and silica components in the starting material, with the  $\alpha$  silicon nitride supplying the nitrogen and the majority of the silicon species necessary for  $\beta$  sialon precipitation. All the  $\beta$  sialon grains precipitated at both  $1500$  and  $1600^\circ\text{C}$  sectioned parallel to the  $c$ -axis have rounded ends. This phenomenon is related to the difference in growth rates parallel and perpendicular to the  $c$ -axis and also to the strain-free liquid environment in which the grains were precipitated and have grown [6]. This rounded growth front is not usually seen in the low glass content sialon ceramics, see Fig. 1, due to impingement of the surrounding  $\beta$  grains.

#### 4. Conclusions

Analysis of the  $\alpha$  to  $\beta$  phase transformation which occurs in silicon nitride-based ceramics was made possible by TEM and SEM using materials containing high proportions of liquid-forming additives. This allowed production of dense samples containing partially transformed  $\alpha$  silicon nitride and also separated the dissolving and precipitating grains making analysis easier.

Pictographical evidence of the  $\alpha$  to  $\beta$  phase transformation was attained which showed dissolving  $\alpha$  silicon nitride particles together with precipitating  $\beta$  sialon crystallites. There appeared to be no preferential dissolution sites on the  $\alpha$  silicon nitride particles.

Diffusion of nitrogen through the liquid phase between the dissolving  $\alpha$  and precipitating  $\beta$  phases must be extremely rapid, because negligible nitrogen was detected in the glassy matrix.

This TEM analysis technique can be used to investigate the effect of different densification oxides on the microstructure of  $\beta$  phase and other sialon materials.

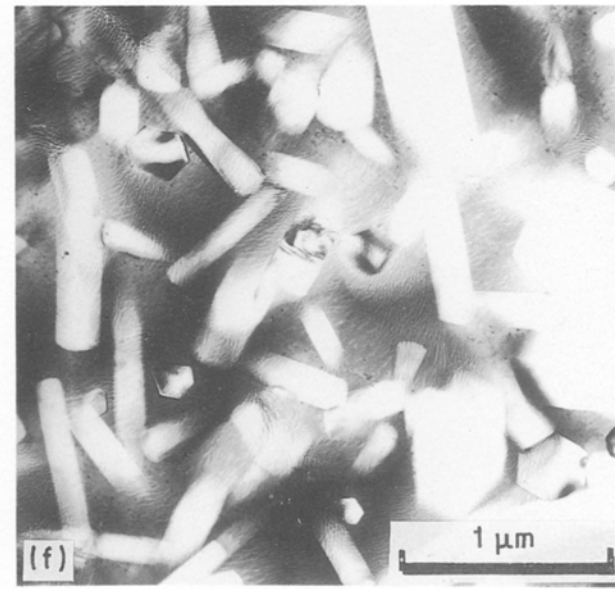
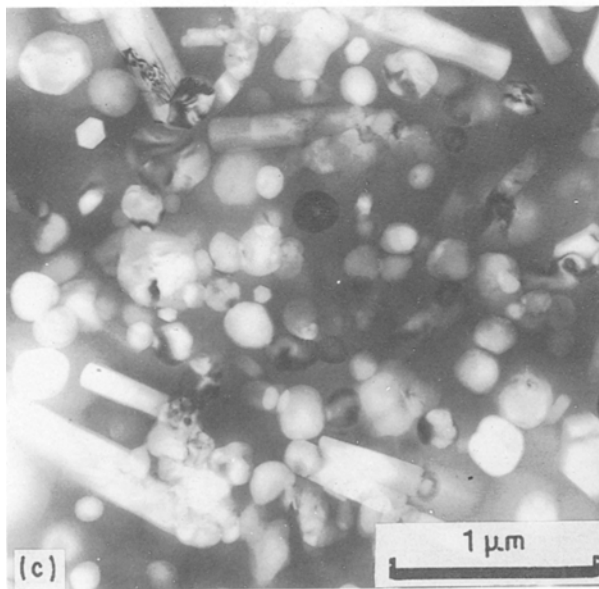
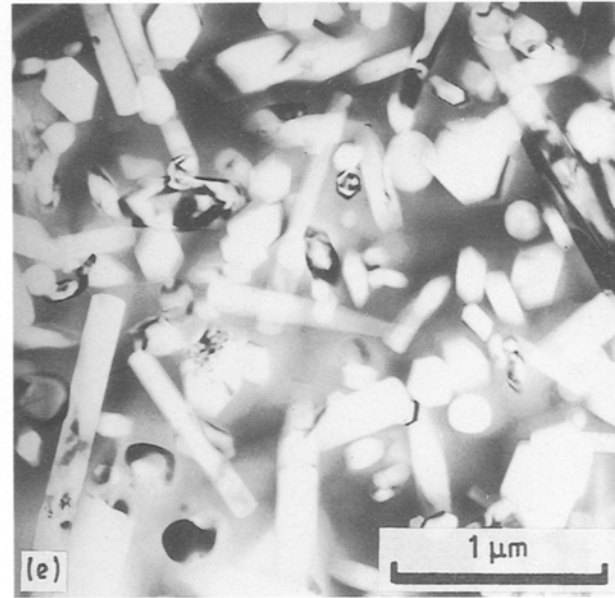
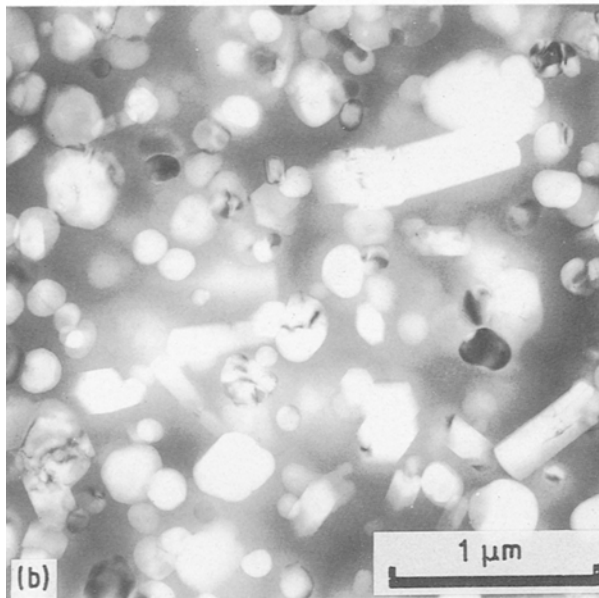
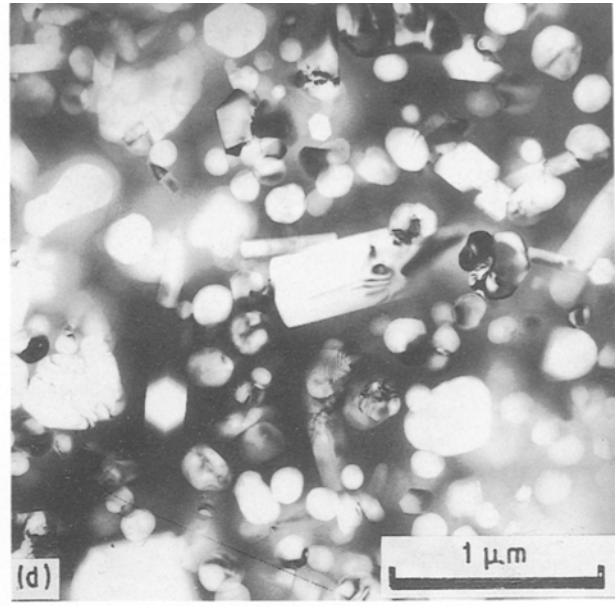
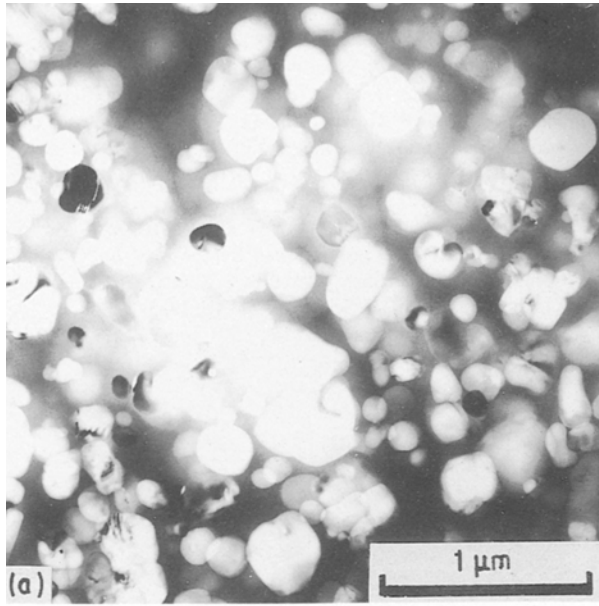


Figure 8 Transmission electron micrographs of Sample C hot-pressed at 1500 °C for (a) 5 min, (b) 10 min and (c) 20 min, and at 1600 °C for (d) 5 min, (e) 10 min and (f) 20 min.

## References

1. W. D. KINGERY, "Ceramic Fabrication Processes" (Wiley, New York, 1959) p. 131.
2. C. WAGNER, *Z. Elektrochem.* **65** (1961) 581.
3. A. J. ARDELL, *Acta Metall.* **20** (1972) 61.
4. S. J. L. KANG, S. M. HAN, D. D. LEE and D. N. YOON, in "Proceedings of the MRS International Meeting on Advanced Materials", Vol. 5, edited by Y. Hamano, O. Kamigaito, T. Kishi and M. Sakai (Materials Research Society, 1989) p. 63.
5. D. D. LEE, S. J. L. KANG, G. PETZOW and D. N. YOON, *J. Amer. Ceram. Soc.* **73** (1990) 767.
6. C. M. HWANG, T. Y. TIEN and I. W. CHEN, in "Sintering '87", Vol. 2, edited by S. Somiya, M. Shimada, M. Yoshimura and R. Watanabe (Elsevier Applied Science, London, (1988) p. 1034.
7. C. M. HWANG and T. Y. TIEN, *Mater. Sci. Forum* **47** (1989) 84.
8. S. HAMPSHIRE, PhD thesis, University of Newcastle-upon-Tyne (1980).
9. D. D. LEE, S. J. L. KANG and D. N. YOON, *J. Amer. Ceram. Soc.* **71** (1988) 803.
10. M. PROKESOVA, *Ceram. Int.* **15** (1989) 369.
11. R. E. LOEHMAN, *J. Non-Cryst. Solids* **42** (1980) 433.
12. P. A. WALLS and D. P. THOMPSON, in "Special Ceramics 8", edited by S. P. Howlett and D. Taylor (Institute of Ceramics, Stoke on Trent, 1986) p. 35.
13. I. A. BONDAR and F. Y. GALAKHOV, *Izv. Akad. Nauk SSSR Ser. Khim.* **7** (1963) 1325.
14. C. SPACIE, N. S. JAMEEL and D. P. THOMPSON, in "Proceedings of the International Symposium on Ceramic Components for Engines", edited by S. Somiya, E. Kanai and K. Ando, Japan (KTK Scientific, Tokyo, 1983) p. 343.
15. S. BOSKOVIC and E. KOSTIC, *Sci. Ceram.* **12** (1984) 391.

*Received 6 March  
and accepted 19 November 1992*